Math. Program., Ser. B (2004)

Digital Object Identifier (DOI) 10.1007/s10107-004-0535-6

Mihai Anitescu · Gary D. Hart

A fixed-point iteration approach for multibody dynamics with contact and small friction

Received: February 22, 2003 / Accepted: June 2, 2004
Published online: ■■ –

Abstract. Acceleration–force setups for multi-rigid-body dynamics are known to be inconsistent for some configurations and sufficiently large friction coefficients (a Painleve paradox). This difficulty is circumvented by time-stepping methods using impulse-velocity approaches, which solve complementarity problems with possibly nonconvex solution sets. We show that very simple configurations involving two bodies may have a nonconvex solution set for any nonzero value of the friction coefficient. We construct two fixed-point iteration algorithms that solve convex subproblems and that are guaranteed, for sufficiently small friction coefficients, to retrieve, at a linear convergence rate, the unique velocity solution of the nonconvex linear complementarity problem whenever the frictionless configuration can be disassembled. In addition, we show that one step of one of the iterative algorithms provides an excellent approximation to the velocity solution of the original, possibly nonconvex, problem if for all contacts we have that either the friction coefficient is small or the slip velocity is small.

Subject Index 70E55, 75M10, 75M15, 90C33

1. Introduction

Multi-rigid-body dynamics with contact and friction is fundamental for virtual reality and robotics simulations. However, the Coulomb model for friction poses several obstacles in the path of efficient simulation. The classical acceleration-force approach does not necessarily have a solution even in the simple case of a rod in contact with a table top at high friction [30, 29]. Recently, time-stepping methods have been developed in an impulse-velocity framework that avoid the inconsistencies that may appear in the classical approach [6, 8, 29, 30]. These methods can be modified to accommodate the most common types of stiffness [7] and are currently investigated in animation [11] and robotics applications [22]. When there is no friction, these time-stepping algorithms solve, at every step, a linear complementarity problem that represents the optimality conditions for a convex quadratic program. When the friction coefficients are nonzero, however, this interpretation is lost and there is no obvious way to guarantee that the solution set is convex, even for small friction coefficients.

In this [1] work we show, with an example, that even a one body on a tabletop configuration may have a nonconvex solution set for arbitrarily small friction coefficients. This

M. Anitescu, G.D. Hart: Department of Mathematics, University of Pittsburgh, Pittsburgh, PA 15260, USA,
e-mail: anitescu@math.pitt.edu, gdhart@pitt.edu

The Mathematics and Computer Science Division, Argonne National Laboratory

[1] A partial version of this work has appeared in the proceedings of the NATO Advanced Studies Institute on Virtual Nonlinear Multibody Systems, Prague, 2002.

is unfortunate, because it seems to indicate that the linear complementarity problem may be hard to solve even for arbitrarily small friction coefficients.

Nevertheless, we show that, for sufficiently small coefficients, the velocity solution is unique whenever the frictionless configuration can be disassembled. The key observation is that, for small friction coefficients at the contacts, the unknown velocity is a fixed point of two contraction mappings. To evaluate the mappings, one needs to solve only one or two convex linear complementarity subproblems (which are the optimality conditions for some convex quadratic program). Therefore, the associated fixed-point iterations have relatively low complexity per iteration.

Several other approaches in computational contact mechanics have a fixed-point iteration flavor where convex subproblems are used to compute the values of the contraction mapping [10, 15, 17, 24, 25]. These approaches evaluate successively the normal force keeping the tangential force fixed and then the tangential force keeping the normal force fixed. The approaches rely fundamentally on the uniqueness of the interaction force for a given configuration, a property that does not hold for our example. So the fixed-point iteration schemes that we propose, which are velocity based, have a broader scope than such force-based iteration methods since they do not require the uniqueness of the interaction force or impulse.

2. The linear complementarity subproblem of the time-stepping scheme

In the following q and, respectively, v constitute the generalized position and, respectively, generalized velocity vector of a system of several bodies [18].

2.1. Model constraints

Our approach covers several types of constraints.

Joint constraints. Such constraints are described by the equations

$$\Theta^{(i)}(q) = 0,\ \ i = 1, 2, \ldots, m\,. \tag{2.1}$$

Here, $\Theta^{(i)}(q)$ are sufficiently smooth functions. We denote by $\nu^{(i)}(q)$ the gradient of the corresponding function, or

$$\nu^{(i)}(q) = \nabla_q \Theta^{(i)}(q), \quad i = 1, 2, \ldots, m.$$

The impulse exerted by a joint on the system is $c_\nu^{(i)} \nu^{(i)}(q)$, where $c_\nu^{(i)}$ is a scalar related to the Lagrange multiplier of classical constrained dynamics [18].

Noninterpenetration constraints. These constraints are defined in terms of a continuous signed distance function between the two bodies $\Phi(q)$ [2]. The noninterpenetration constraints become

$$\Phi^{(j)}(q) \geq 0, \quad j = 1, 2, \ldots, p. \tag{2.2}$$

The function $\Phi(q)$ is generally not differentiable, especially when the bodies have flat surfaces. Usually, this situation is remediable by considering different geometric primitives [13] that result in noninterpenetration constraints being expressed in terms of several inequalities involving differentiable functions $\Phi(q)$. In the following, we may refer to (j) as the *contact (j)*, though the contact is truly active only when $\Phi^{(j)}(q) = 0$. We denote the normal at contact (j) by

$$n^{(j)}(q) = \nabla_q \Phi^{(j)}(q), \ \ j = 1, 2, \dots, p. \tag{2.3}$$

When the contact is active, it can exert a compressive normal impulse, $c_n^{(j)} n^{(j)}(q)$ on the system, which is quantified by requiring $c_n^{(j)} \geq 0$. The fact that the contact must be active before a nonzero compression impulse can act is expressed by the complementarity constraint

$$\begin{aligned} \Phi^{(j)}(q) &\geq 0, \\ c_n^{(j)} &\geq 0, \ \ j = 1, 2, \dots, p, \\ \Phi^{(j)}(q) c_n^{(j)} &= 0. \end{aligned} \tag{2.4}$$

Frictional constraints. These are expressed by means of a discretization of the friction cone [7, 6, 30]. For a contact j, we take a collection of coplanar vectors $d_i(q)$, $i = 1, 2, \dots, m_C$, which span the plane tangent at the contact (though the plane may cease to be tangent to the contact normal when mapped in generalized coordinates [2]). The cover of the vectors $d_i(q)$ should approximate the transversal shape of the friction cone. In two-dimensional mechanics, the tangent plane is one dimensional, its transversal shape is a segment, and only two such vectors $d_1(q)$ and $d_2(q)$ are needed in this formulation. We denote by $D(q)$ a matrix whose columns are $d_i(q)$, $i = 1, 2, \dots, m_C$, or $D(q) = \left[d_1(q), d_2(q), \dots, d_{m_C}(q)\right]$. A tangential impulse is $\sum_{i=1}^{m_C} \beta_i d_i(q)$, where $\beta_i \geq 0$, $i = 1, 2, \dots, m_C$. We assume that the tangential contact description is symmetric, that is, that for any i there exists a j such that $d_i(q) = -d_j(q)$.

The friction model ensures maximum dissipation for given normal impulse c_n and velocity v and guarantees that the total contact force is inside the discretized cone. We express this model as

$$\begin{aligned} D(q)^T v + \lambda e \geq 0 \perp \beta \geq 0, \\ \mu c_n - e^T \beta \geq 0 \perp \lambda \geq 0. \end{aligned} \tag{2.5}$$

Here e is a vector of ones of dimension m_C, $e = (1, 1, \dots, 1)^T$, μ is the friction parameter, and β is the vector of tangential forces $\beta = \left(\beta_1, \beta_2, \dots, \beta_{m_C}\right)$. The additional variable λ is approximately equal to the norm of the tangential velocity at the contact, if there is relative motion at the contact, or $\|D(q)^T v\| \neq 0$ [6, 30].

Notations. We denote by $M(q)$ the symmetric, positive definite, mass matrix of the system in the generalized coordinates q and by $k(t, q, v)$ the external force. All quantities described in this section associated with contact j are denoted by the superscript $^{(j)}$. When we use a vector or matrix norm whose index is not specified, it is the 2-norm.

2.2. The linear complementarity problem

To include these constraints in a time-stepping scheme, we formulate all geometrical constraints at the velocity level by linearization. To this end we assume that at the current time step we have exact feasibility of the noninterpenetration and joint constraints. This assumption can be practically satisfied if at the end of each integration step we do a projection onto the feasible manifold [7]. Projection methods have been successfully used for constraint stabilization for differential algebraic equations, and can be shown to not affect the order of convergence [9]. For finite time steps, however, projection methods could have the unfortunate side effect of substantially altering the energy of the system, when stiff forces are present. Nevertheless, for the special (and very common) case of stiff forces originating in springs and dampers, we have shown that the projection method can be modified by including constraints that depend on the spring configuration in such a fashion that stiffness is accommodated and the energy balance of the time-stepping scheme is not altered [7].

Let h be the time step. If, at some time $t^{(l)}$, the system is at position $q^{(l)}$ and velocity $v^{(l)}$, then we choose the new position to be $q^{(l+1)} = q^{(l)} + hv^{(l+1)}$, where $v^{(l+1)}$ is determined by enforcing the simulation constraints. For joint constraints the linearization leads to $\nabla_q \Theta^{(i)^T}(q^{(l)})v^{(l+1)} = \nu^{(i)^T}(q^{(l)})v^{(l+1)} = 0$ for $i = 1, 2, \dots, m$. For noninterpenetration constraint j, $\Phi^{(j)}(q) \geq 0$, where $j = 1, 2, \dots, p$, linearization at $q^{(l)}$ for one time step amounts to $\Phi^{(j)}(q^{(l)}) + h\nabla_q \Phi^{(j)^T}(q^{(l)})v^{(l+1)} \geq 0$, that is,

$$n^{(j)^T}(q^{(l)})v^{(l+1)} + \frac{\Phi^{(j)}(q^{(l)})}{h} = \nabla_q \Phi^{(j)^T}(q^{(l)})v^{(l+1)} + \frac{\Phi^{(j)}(q^{(l)})}{h} \geq 0. \tag{2.6}$$

Since we assume that at step (l) all geometrical constraints are satisfied, this implies that $\frac{\Phi^{(j)}(q^{(l)})}{h} \geq 0$. For computational efficiency, only the contacts that are imminently active are included in the dynamical resolution and linearized, and their set is denoted by $\mathcal{A}$. One practical way of determining $\mathcal{A}$ is by including all j for which $\Phi^{(j)}(q) \leq \delta$, where δ is a sufficiently small quantity, perhaps dependent on the size of the velocity.

If a contact j switches from inactive to active (the corresponding $c_n^{(j)}$ is positive), a collision resolution, possibly with energy restitution, needs to be applied [6]. In this work we consider only totally plastic collisions, where no energy lost during collision is restituted. Therefore we avoid the need to consider a compression followed by decompression linear complementarity problem, as is done in certain approaches [6].

After collecting all the constraints introduced above, with the geometrical constraints replaced by their linearized versions, we obtain the following mixed linear complementarity problem.

$$\begin{bmatrix} M^{(l)} & -\widetilde{\nu} & -\widetilde{n} & -\widetilde{D} & 0 \\ \widetilde{\nu}^T & 0 & 0 & 0 & 0 \\ \widetilde{n}^T & 0 & 0 & 0 & 0 \\ \widetilde{D}^T & 0 & 0 & 0 & \widetilde{E} \\ 0 & 0 & \widetilde{\mu} & -\widetilde{E}^T & 0 \end{bmatrix} \begin{bmatrix} v^{(l+1)} \\ c_\nu \\ c_n \\ \widetilde{\beta} \\ \lambda \end{bmatrix} + \begin{bmatrix} -Mv^{(l)} - hk^{(l)} \\ 0 \\ \Delta \\ 0 \\ 0 \end{bmatrix} = \begin{bmatrix} 0 \\ 0 \\ \rho \\ \widetilde{\sigma} \\ \zeta \end{bmatrix} \tag{2.7}$$

$$\begin{bmatrix} c_n \\ \widetilde{\beta} \\ \lambda \end{bmatrix}^T \begin{bmatrix} \rho \\ \widetilde{\sigma} \\ \zeta \end{bmatrix} = 0, \qquad \begin{bmatrix} c_n \\ \widetilde{\beta} \\ \lambda \end{bmatrix} \geq 0, \qquad \begin{bmatrix} \rho \\ \widetilde{\sigma} \\ \zeta \end{bmatrix} \geq 0 . \tag{2.8}$$

Here $\widetilde{\nu} = [\nu^{(1)}, \nu^{(2)}, \ldots, \nu^{(m)}], c_\nu = [c_\nu^{(1)}, c_\nu^{(2)}, \ldots, c_\nu^{(m)}]^T, \widetilde{n} = [n^{(j_1)}, n^{(j_1)}, \ldots, n^{(j_s)}]$, $c_n = [c_n^{(j_1)}, c_n^{(j_2)}, \ldots, c_n^{(j_s)}]^T, \widetilde{\beta} = [\beta^{(j_1)T}, \beta^{(j_2)T}, \ldots, \beta^{(j_s)T}], \widetilde{D} = [D^{(j_1)}, D^{(j_2)}, \ldots,$ $D^{(j_s)}], \lambda = [\lambda^{(j_1)}, \lambda^{(j_2)}, \ldots, \lambda^{(j_s)}], \widetilde{\mu} = diag(\mu^{(j_1)}, \mu^{(j_2)}, \ldots, \mu^{(j_s)})^T, \Delta = \frac{1}{h}\left(\Phi^{(j_1)},\right.$ $\left.\Phi^{(j_2)}, \ldots, \Phi^{(j_s)}\right)^T$ and

$$\widetilde{E} = \begin{bmatrix} e^{(j_1)} & 0 & 0 \cdots & 0 \\ 0 & e^{(j_2)} & 0 \cdots & 0 \\ \vdots & \vdots & \vdots \; \vdots & \vdots \\ 0 & 0 & 0 \cdots & e^{(j_s)} \end{bmatrix}$$

are the lumped LCP data, and $\mathcal{A} = \{j_1, j_2, \ldots, j_s\}$ are the active contact constraints. The vector inequalities in (2.8) are to be understood component wise. We use the ˜ notation to indicate that the quantity is obtained by properly adjoining blocks that are relevant to the aggregate joint or contact constraints.

To simplify the presentation we do not explicitly include the dependence of the geometrical parameters on the data of the simulation. Also $M^{(l)} = M(q^{(l)})$ is the mass matrix, which from our assumption is positive definite, for any l , and $k^{(l)} = k(t^{(l)}, q^{(l)}, v^{(l)})$ represents the external force at time (l). Note that, since $\Delta \geq 0$, the results from [6] can be applied to show that the above linear complementarity problem is guaranteed to have a solution, without any further assumptions. For the case where the pointed friction cone assumption holds, very general existence results (that do not necessarily require $\Delta \geq 0$) can be obtained from [26].

2.3. Background

To establish our convergence results, we use several previous results, some of which we include in this section for completeness.

2.3.1. Pointed friction cone. To obtain good properties of this new mixed linear complementarity problem and a good approximation of the original mixed linear complementarity problem (2.7–2.8), we make a friction cone regularity assumption. We define the friction cone to be the portion in the configuration space that can be covered by feasible constraint interaction forces, or

$$FC(q) = \left\{ t = \tilde{\nu} c_\nu + \tilde{n} c_n + \tilde{D}\tilde{\beta} \,\middle|\, c_n \geq 0,\ \tilde{\beta} \geq 0,\ \|\beta^{(j)}\|_1 \leq \mu^{(j)} c_n^{(j)},\ \forall j \in \mathcal{A} \right\}. \tag{2.9}$$

Clearly, the cone $FC(q)$ is a convex set.

Definition.

$$\begin{aligned} &\textit{We say that FC(q) is pointed} \Leftrightarrow \forall \left(c_\nu, c_n \geq 0, \tilde{\beta} \geq 0 \right) \neq 0 \\ &\qquad \textit{such that } \|\beta^{(j)}\|_1 \leq \mu^{(j)} c_n^{(j)}, \forall j \in \mathcal{A} \\ &\qquad \textit{we must have that } \tilde{\nu} c_\nu + \tilde{n} c_n + \tilde{D}\tilde{\beta} \neq 0. \end{aligned} \tag{2.10}$$

For the case where the geometrical constraints consist only of noninterpenetration constraints, this definition is equivalent to requiring that $FC(q)$ contain no proper linear subspace [29]. The pointed friction cone assumption is essential in ensuring that the limits of the solutions of the time-stepping scheme (2.7–2.8) converge to a weak solution of the continuous problem [29].

Of particular interest is the description of the pointedness of the friction cone when the friction coefficients are zero, that is $\tilde{\mu} = 0$. Using duality as in the relationship between MFCQ and (2.13), we can see that the set of friction coefficients diag $(\tilde{\mu})$ for which the friction cone is pointed forms an open set. Therefore, pointedness of the friction cone for the frictionless case $\tilde{\mu} = 0$ also implies pointedness of the friction cone for small values of the friction coefficients. This observation is essential in stating our small friction results.

It is also of interest to write an alternative description of the pointedness of the friction cone for the frictionless case. By specializing (2.10) for the case where $\tilde{\mu} = 0$, we obtain

$$\tilde{n} c_n + \tilde{\nu} c_\nu = 0, \ c_n \geq 0 \Rightarrow c_n = 0, \ c_\nu = 0. \tag{2.11}$$

Using duality in the same way we did to uncover the relationship between MFCQ and (2.13), we can determine that this description is equivalent to the joint constraint matrix $\tilde{\nu}$ having linearly independent columns and

$$\exists v \text{ such that } \tilde{\nu}^T v = 0 \text{ and } \tilde{n}^T v > 0.$$

The latest condition means that the rigid body configuration can be disassembled [3]: there exists an external force that breaks all contacts while keeping feasibility of the joint constraints. This condition can be established visually for most simple configurations.

2.3.2. Lipschitz stability of strictly convex quadratic programs. In this work, we use several well-known results concerning Lipschitz stability of the solution of strictly convex quadratic programs with respect to perturbation parameters. Some of these results are stated through similar properties of nonlinear programs.

For a nonlinear program depending on parameters a,

$$\begin{array}{rl} \min_x & f(x,a) \\ \text{subject to} & g_i(x,a) \leq 0 \ \ i = 1, 2, \ldots, m \\ & h_j(x,a) = 0 \ \ j = 1, 2, \ldots, r \end{array} \tag{2.12}$$

the key to obtaining Lipschitz continuity results of the solution x^* as a function of a is to have a constraint qualification at the solution.

At a point x (which may be infeasible) we denote by $\mathcal{B}$ the active set:

$$\mathcal{B}(x,a) = \{ i = 1, 2, \ldots, m | g_i(x,a) \geq 0 \}.$$

We say that (2.12) satisfies the Mangasarian-Fromovitz constraint qualification at x if [20, 21]

$$\text{(MFCQ)} \qquad \begin{array}{l} 1.\ \nabla_x h_j(x,a),\ \ j = 1,2,\ldots,r,\ \text{ are linearly independent and} \\ 2.\ \exists p \neq 0\ \text{ such that }\ \nabla_x h_j(x,a)^T p = 0, \quad j = 1,2,\ldots,r \\ \text{and }\ \nabla_x g_i(x,a)^T p < 0, \quad i \in \mathcal{B}(x,a). \end{array}$$

A very useful characterization of the case when MFCQ does not hold is given by an alternative theorem [12], which states that MFCQ does not hold at a point x for NLP if and only if

$$\begin{array}{c} \exists 0 \neq (\eta,\zeta) \in I\!R^m \times I\!R^r,\ \eta \geq 0; \quad \eta_i = 0, \eta \notin \mathcal{B}(x,a) \text{ such that} \\ \sum_{i \in \mathcal{B}(x,a)} \eta_i \nabla_x g_i(x,a) + \sum_{j=1}^r \zeta_j \nabla_x h_j(x,a) = 0. \end{array} \tag{2.13}$$

The key result we use here is due to Robinson [27]. If MFCQ and certain strong second-order conditions hold (which are satisfied by quadratic programs with a symmetric positive definite matrix) at a solution x^* for a choice of parameters a_0, then there exist a parameter L, a neighborhood $\mathcal{V}(x^*)$ of x^* and $\mathcal{V}(a_0)$ of a_0 such that for any $a \in \mathcal{V}(a_0)$ the nonlinear program (2.12) has a unique solution $x(a) \in \mathcal{V}(x^*)$ and for any $a_1, a_2 \in \mathcal{V}(a_0)$ we have

$$\|x(a_1) - x(a_2)\| \leq L\|a_1 - a_2\|.$$

Solutions with this property are said to be locally Lipschitz continuous.

The Lipschitz continuity property can subsequently be strengthened even in the absence of MFCQ for quadratic programs that are perturbed only in the right-hand side of the constraints [12, Problem 7.6.10]

Theorem 1. *Consider the quadratic program*

$$\begin{array}{ll} \textit{minimize} & q^T x + \frac{1}{2} x^T Q x \\ \textit{subject to} & Ax \geq a \\ & Bx = b \end{array}$$

where the matrix Q is assumed symmetric positive definite. Let $x(q,a,b)$ denote the unique solution of this quadratic program if it exists. Then there exists a parameter $L \geq 0$ such that for any two pairs of vectors (q,a,b) and (q',a',b'), we have

$$\|x(q,a,b) - x(q',a',b')\| \leq L\|(q,a,b) - (q',a',b')\|,$$

if both $x(q,a,b)$ and $x(q',a',b')$ exist.

3. An example of configuration with nonconvex solution set

If the friction coefficients are $\mu^{(j)} = 0$, $j \in \mathcal{A}$, then the mixed linear complementarity problem (2.7–2.8) has a positive semidefinite matrix and can be shown to always have a convex solution set. Such mixed linear complementarity problems can be solved in a time that is polynomial with respect to the problem size [5]. Polynomial complexity is almost always associated with the convexity of the solution set of (2.7–2.8), which, as we now show, may not occur for any positive friction coefficients.

Consider the configuration in Figure 1, where a body of mass m, shaped like a hexagonal pyramid, is in contact with a fixed tabletop (whose edges are not shown) in the position shown, for which we are going to set up the linear complementarity problem (2.7–2.8). In the following description we represent all relevant vectors with respect to the three-dimensional space. The generalized coordinates [18] consist of the three translational coordinates and three rotational coordinates of the body about its center of mass C.

The contact configuration is represented by six point-on-plane contact constraints [2], one for each corner of the pyramid in contact with the tabletop. The friction coefficient μ is the same for all contact constraints. At each corner, we use a four-faceted pyramidal approximation of the friction cone ($m_C^{(j)} = 4$, $j = 1, 2, \dots, 6$). The directions used for the pyramidal approximation of the friction cone are $w_1 = (1, 0, 0)^T$ and $w_2 = (0, 1, 0)^T$. The normal at each contact in global coordinates is $n = (0, 0, 1)^T$. From the center of mass C we have six vectors, $p^{(j)}$, $j = 1, 2, \dots, 6$, pointing toward the six bottom vertices of the pyramid and whose projection on the contact plane between the pyramid and the tabletop are $r^{(j)}$, $j = 1, 2, \dots, 6$. Note that $p^{(j)} \times n = r^{(j)} \times n$, for $j = 1, 2, \dots, 6$, where $\times$ denotes the vector product. We assume that the bottom of the pyramid is a regular hexagon, which means that we have

$$r^{(1)} + r^{(3)} + r^{(5)} = 0, \quad r^{(2)} + r^{(4)} + r^{(6)} = 0. \tag{3.14}$$

We now construct the generalized representations of the vectors that are normal and tangent to the contacts in global coordinates. We have that [2] (refer to Section 2 for the choice of notation)

$$\begin{aligned} n^{(j)} &= \begin{pmatrix} n \\ r^{(j)} \times n \end{pmatrix}, \\ d_i^{(j)} &= \begin{pmatrix} w_i \\ p^{(j)} \times w_i \end{pmatrix}, \; d_{i+2}^{(j)} = -d_i^{(j)}, \quad i = 1, 2, \quad j = 1, 2, \dots, 6. \end{aligned} \tag{3.15}$$

From the expression of the generalized normals and (3.14) we obtain

$$n^{(1)} + n^{(3)} + n^{(5)} = 3 \begin{pmatrix} n \\ \mathbf{0}_3 \end{pmatrix}, \quad n^{(2)} + n^{(4)} + n^{(6)} = 3 \begin{pmatrix} n \\ \mathbf{0}_3 \end{pmatrix}. \tag{3.16}$$

The mass matrix with respect to the generalized coordinates for this one-body configuration (since the tabletop is assumed to be sufficiently extended and fixed with respect to the three-dimensional space) is

$$M = \left(\begin{array}{ccc|c} m & 0 & 0 & \\ 0 & m & 0 & \mathbf{0}_{3\times 3} \\ 0 & 0 & m & \\ \hline \multicolumn{3}{c|}{\mathbf{0}_{3\times 3}} & J \end{array} \right),$$

where J is the inertia matrix, which we assume to be symmetric positive definite.

We assume that the initial velocity of this configuration, $v^{(0)}$, is 0. We analyze one time step based on (2.7–2.8) starting at time 0 and with time step h. We denote by g

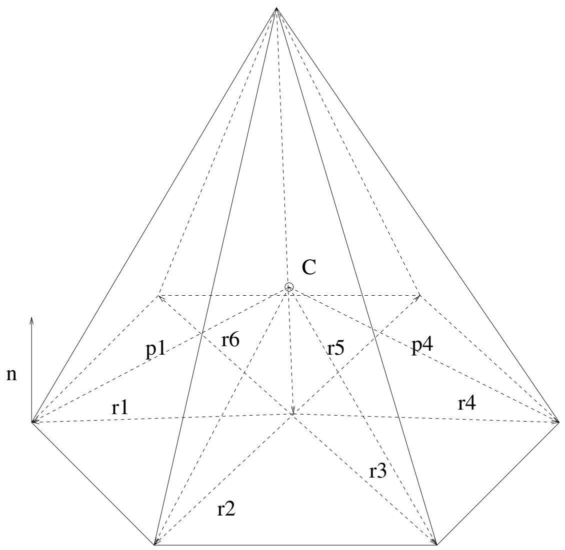

Fig. 1. Example with a nonconvex solution set

the magnitude of the gravitational acceleration, and we assume that gravity is the only external force acting on the body. Since we can assume that gravity acts at the center of mass C in a direction opposed to the vector n, the external force k becomes

$$k = -g \begin{pmatrix} n \\ \mathbf{0}_3 \end{pmatrix}$$

in global generalized coordinates.

We now replace all the above defined quantities in (2.7–2.8). We expect that one possible outcome is $v^{(1)} = 0$, or that the body does not move (the uniqueness of this solution, at least for small μ, will be proved later). We attempt to find a solution of (2.7–2.8) that has zero tangential force, or $\beta_i^{(j)} = 0$, $i = 1, 2, 3, 4$, $j = 1, 2, \ldots, 6$. When this ansatz is replaced in (2.7–2.8), the constraints that remain to be satisfied are

$$\begin{aligned} \textstyle\sum_{j=1}^{6} c_n^{(j)} n^{(j)} - hmg \begin{pmatrix} n \\ \mathbf{0}_3 \end{pmatrix} &= 0. \\ \mu c_n^{(j)} \geq 0 \perp \lambda^{(j)} \geq 0, \quad j &= 1, 2, \ldots, 6. \end{aligned}$$

Using (3.16), we have the following choices that satisfy these constraints, and, thus, constitute a part of the solution: of (2.7–2.8)

1. $c_n^{(1)} = c_n^{(3)} = c_n^{(5)} = \frac{hmg}{3}$, $c_n^{(2)} = c_n^{(4)} = c_n^{(6)} = 0$, $\lambda^{(1)} = \lambda^{(3)} = \lambda^{(5)} = 0$, $\lambda^{(2)} = \lambda^{(4)} = \lambda^{(6)} = 1$,
2. $c_n^{(1)} = c_n^{(3)} = c_n^{(5)} = 0$, $c_n^{(2)} = c_n^{(4)} = c_n^{(6)} = \frac{hmg}{3}$, $\lambda^{(1)} = \lambda^{(3)} = \lambda^{(5)} = 1$, $\lambda^{(2)} = \lambda^{(4)} = \lambda^{(6)} = 0$.

If, however, we take the average of the solutions, we obtain that $c_n^{(j)} = \frac{hmg}{6}$, $\lambda^{(j)} = \frac{1}{2}$, for $j = 1, 2, \ldots, 6$, which violate the complementarity constraint

$$\mu c_n^{(j)} \geq 0 \ \perp \ \lambda^{(j)} \geq 0, \quad j = 1, 2, \ldots, 6,$$

as soon as $\mu > 0$ (the rest of the constraints must be satisfied because they are linear). This implies that the solution set of (2.7–2.8) is not convex.

Therefore, even for simple cases and arbitrarily small but nonzero friction coefficients, the solution set of (2.7–2.8) cannot be expected to be convex. Hence the matrix of this linear complementarity problem cannot be P_* [19]. The P_* class is the largest matrix class for which polynomial time algorithms are known for linear complementarity problems [19] or mixed linear complementarity problems [5].

This raises an important difficulty in the path of efficiently finding solutions to the multibody dynamics problem with contact and friction, when a considerable number of contacts is active, even at small friction coefficients.

To address this problem, in the following sections we develop two iterative methods that have a guaranteed rate of convergence to the velocity solution of (2.7–2.8) for sufficiently small but nonzero friction coefficients. The methods have convex subproblems that can be solved in polynomial time.

4. Convex relaxation of (2.7–2.8)

We now investigate a convex relaxation of (2.7–2.8), with the ultimate purpose of setting up a fixed-point iteration that converges to its solution, at least for small values of the friction coefficient. The relaxation modifies the linearization of the noninterpenetration constraint. A related LCP relaxes the relationship between the sizes of the normal and the tangential contact impulses and can be used in conjunction with the first relaxation to set up a fixed-point iteration whose iterates do not exhibit the normal velocity drift of the first case. To simplify notation, we replace the superscript $(l+1)$ of the velocity solution of (2.7–2.8) by $*$, and we use no superscript when defining the complementarity problems.

4.1. A strictly convex quadratic program relaxation of (2.7–2.8)

We first approximate the mixed linear complementarity problem (2.7–2.8) by the following mixed linear complementarity problem:

$$\begin{bmatrix} M^{(l)} & -\widetilde{\nu} & -\widetilde{n} & -\widetilde{D} & 0 \\ \widetilde{\nu}^T & 0 & 0 & 0 & 0 \\ \widetilde{n}^T & 0 & 0 & 0 & -\widetilde{\mu} \\ \widetilde{D}^T & 0 & 0 & 0 & \widetilde{E} \\ 0 & 0 & \widetilde{\mu} & -\widetilde{E}^T & 0 \end{bmatrix} \begin{bmatrix} v \\ c_\nu \\ c_n \\ \widetilde{\beta} \\ \lambda \end{bmatrix} + \begin{bmatrix} -Mv^{(l)} - hk^{(l)} \\ \Upsilon \\ \Gamma + \Delta \\ 0 \\ 0 \end{bmatrix} = \begin{bmatrix} 0 \\ 0 \\ \rho \\ \widetilde{\sigma} \\ \zeta \end{bmatrix} \tag{4.17}$$

$$\begin{bmatrix} c_n \\ \widetilde{\beta} \\ \lambda \end{bmatrix}^T \begin{bmatrix} \rho \\ \widetilde{\sigma} \\ \zeta \end{bmatrix} = 0, \qquad \begin{bmatrix} c_n \\ \widetilde{\beta} \\ \lambda \end{bmatrix} \geq 0, \qquad \begin{bmatrix} \rho \\ \widetilde{\sigma} \\ \zeta \end{bmatrix} \geq 0\,. \tag{4.18}$$

Clearly, the matrix of the linear complementarity problem, is now positive semidefinite. Here $\Gamma = \left(\Gamma^{(j_1)}, \Gamma^{(j_2)}, \ldots, \Gamma^{(j_s)}\right)^T$ is a nonnegative vector that has as many components as active constraints (elements in $\mathcal{A}$) and $\Upsilon = 0$. We introduce the parameter Υ in order to maintain the full generality of our following sensitivity results. The fact that $\Delta \geq 0$ and $\Upsilon = 0$ will be used only when needed, and some of our results will be stated without any restriction on Δ and Υ.

Very useful results can be obtained based on the interpretation of (4.17–4.18) as a a quadratic program. To simplify the notation, we denote by $q^{(l)} = -Mv^{(l)} - hk^{(l)}$. We now have our mixed complementarity problem (4.17–4.18) in the form

$$\begin{array}{lllll} M^{(l)}v & -\widetilde{n}\widetilde{c}_n & -\widetilde{D}\widetilde{\beta} & & = -q^{(l)} \\ \widetilde{\nu}^T v & & & & = -\Upsilon \\ \widetilde{n}^T v & & & -\tilde{\mu}\lambda & \geq -\Gamma - \Delta \perp c_n \geq 0 \\ \widetilde{D}^T v & & & +\widetilde{E}\lambda & \geq 0 \quad\quad\quad \perp \widetilde{\beta} \geq 0 \\ & \tilde{\mu}c_n & -\widetilde{E}^T\widetilde{\beta} & & \geq 0 \quad\quad\quad \perp \lambda \geq 0. \end{array} \tag{4.19}$$

Lemma 1. *Assume that $\Upsilon = 0$. If for a solution $\left(v^*, c_\nu, c_n, \tilde{\beta}, \lambda\right)$ of (4.19) we have that $\Gamma = \tilde{\mu}\lambda$, then that solution of (4.19) is a solution of (2.7–2.8). Conversely, any solution $\left(v^*, c_\nu, c_n, \tilde{\beta}, \lambda\right)$ of (2.7–2.8) is a solution of (4.17–4.18) with $\Gamma = \tilde{\mu}\lambda$.*

Proof. The proposed substitution makes the two LCPs identical. □

Note that (4.19) can be seen as constituting the first-order optimality conditions of the quadratic program

$$\begin{array}{lll} \min_{v,\lambda} & \frac{1}{2}v^T M^{(l)} v + q^{(l)^T} v & \\ \text{subject to} & n^{(j)^T} v - \mu^{(j)}\lambda^{(j)} \geq -\Gamma^{(j)} - \Delta^{(j)}, & j \in \mathcal{A} \\ & D^{(j)^T} v + \lambda^{(j)} e^{(j)} \geq 0, & j \in \mathcal{A} \\ & \nu_i^T v = -\Upsilon_i, & i = 1, 2, \ldots, p \\ & \lambda^{(j)} \geq 0 & j \in \mathcal{A}. \end{array} \tag{4.20}$$

Lemma 2. *Any solution (v, λ) of (4.20), together with its Lagrange multipliers, is a solution of the linear complementarity problem (4.17–4.18). Conversely, the v, λ components of any solution of (4.17–4.18) are a solution of (2).*

Proof. If we write out the first-order optimality conditions for (4.20), we get (4.19). The result is true by the property of first-order optimality conditions and by the convexity of the quadratic program (4.20). □

The quadratic program (4.20) is not strictly convex with respect to the ensemble of the variables (v, λ), but it is strictly convex with respect to v. By using the two inequalities involving λ, and that each tangential description of the contact is symmetric, we are able to show that v is in effect the unique solution of the following strictly convex quadratic program:

$$\begin{array}{lll} \min_v & \frac{1}{2}v^T M^{(l)} v + q^{(l)^T} v & \\ \text{subject to} & e^{(j)} n^{(j)^T} v + \mu^{(j)} D^{(j)^T} v \geq -\left(\Gamma^{(j)} + \Delta^{(j)}\right) e^{(j)}, & j \in \mathcal{A} \\ & \nu_i^T v = -\Upsilon_i, & i = 1, 2, \ldots, p \end{array} \tag{4.21}$$

If we assume that $\Gamma \geq 0$, $\Delta \geq 0$ and $\Upsilon_i = 0$, it immediately follows that this quadratic program is feasible, because $v = 0$ is a feasible point. Moreover, whenever it is feasible, it has a unique solution $v^*(\Gamma)$, since we assume that $M^{(l)}$ is positive definite. This allows us to introduce the mapping

$$P_1(\Gamma) = v^*(\Gamma). \tag{4.22}$$

which is well-defined for any Γ for which (4.21) is feasible.

Let v be a velocity vector. For the given active set $\mathcal{A}$, another useful function that we define is

$$\Lambda(v) = \lambda, \tag{4.23}$$

where

$$\lambda^{(j)} = \max_{i=1,2,\ldots,m_C^{(j)}} \left\{ d_i^{(j)^T}(v) \right\}, \quad j \in \mathcal{A}.$$

Because of the way $D^{(j)}$ is balanced for a given contact j, there are two immediate items to note. First, for any fixed v, $\Lambda(v) \geq 0$. Second, $\Lambda(v)$ produces the smallest possible λ that satisfies the equation

$$\widetilde{D}^T v + \widetilde{E}\lambda \geq 0.$$

After $v^*(\Gamma)$ is found, then a λ^*, that, together with $v^*(\Gamma)$, is a solution of (4.20) can be found by choosing

$$\lambda^* = \Lambda(v^*). \tag{4.24}$$

Therefore, all the properties of the velocity solution of (4.17–4.18) can be inferred by working with (4.21), once we show that the two problems have the same v-solution. The quantity λ^* is implicitly a function of Γ, but, for defining its properties, we prefer to regard λ^* as a function of v^*, or $\lambda^*(v^*)$.

Theorem 2. *Whenever (4.20) is feasible, the v-solution of (4.20) is unique and is, in fact, a solution of (4.21). Conversely, if v is a solution of (4.21), then $(v, \Lambda(v))$ is a solution of (4.20).*

Proof. Let (v_2, λ_2) be a solution to (4.20). Therefore, we have

$$n^{(j)^T} v_2 - \mu^{(j)} \lambda_2^{(j)} \geq -\Gamma^{(j)} - \Delta^{(j)}, \quad j \in \mathcal{A}$$

and

$$D^{(j)^T} v_2 + e^{(j)} \lambda_2^{(j)} \geq 0, \quad j \in \mathcal{A},$$

from which it follows, by multiplying the second inequality by $\mu^{(j)}$ and adding it componentwise to the first inequality, that

$$e^{(j)} n^{(j)^T} v_2 + \mu^{(j)} D^{(j)^T} v_2 \geq -e^{(j)} \left(\Gamma^{(j)} + \Delta^{(j)} \right), \quad j \in \mathcal{A}.$$

Hence, v_2 is feasible for (4.21), which must now have an optimal solution v_1 that satisfies

$$\frac{1}{2}{v_1}^T M^{(l)} v_1 + q^T v_1 \leq \frac{1}{2}{v_2}^T M^{(l)} v_2 + q^T v_2.$$

On the other hand, the solution of (4.21) satisfies

$$e^{(j)} {n^{(j)}}^T v_1 + \mu^{(j)} {D^{(j)}}^T v_1 \geq -e^{(j)} \left(\Gamma^{(j)} + \Delta^{(j)}\right), \quad j \in \mathcal{A}. \tag{4.25}$$

Define $\lambda_1 = \Lambda(v_1)$, so, by (4.23), we have that

$${D^{(j)}}^T v_1 + e^{(j)} \lambda_1^{(j)} \geq 0, \; j \in \mathcal{A}. \tag{4.26}$$

Also, from (4.23) and the fact that the columns of $D^{(j)}$ form a balanced set, we must have that ${d_i^{(j)}}^T v_1 + \lambda_1^{(j)} = 0$ for some i among $1, 2, \ldots, m_C^{(j)}$. Since from (4.25) we must have that ${n^{(j)}}^T v_1 + \mu^{(j)} {d_i^{(j)}}^T v_1 \geq -\left(\Gamma^{(j)} + \Delta^{(j)}\right)$, the last equality implies

$${n^{(j)}}^T v_1 - \mu^{(j)} \lambda_1^{(j)} \geq -\left(\Gamma^{(j)} + \Delta^{(j)}\right), \, j \in \mathcal{A}$$

and thus from (4.26) we obtain that (v_1, λ_1) is feasible for (4.20). Hence

$$\frac{1}{2}{v_2}^T M^{(l)} v_2 + q^T v_2 \leq \frac{1}{2}{v_1}^T M^{(l)} v_1 + q^T v_1.$$

Therefore, the objective functions of (4.20) and (4.21) must be equal to each other. That means $(v_1, \Lambda(v_1))$ is optimal for (4.20) and v_2 is optimal for (4.21). The proof is complete upon recalling the uniqueness of the solution of (4.21). □

The matrix of the quadratic program (4.20) is clearly not positive definite with respect to the ensemble (v, λ) of the variables. Therefore we do not expect the solution of (4.20) to be unique. We have shown, however, that the velocity component of (4.20), as a result of its equivalence with (4.21) from Theorem 2, is indeed unique, and the block matrix associated with the velocity is positive definite. There may be multiple λ solutions, but there exists a minimal choice $\lambda = \Lambda(v)$ that regularizes the problem.

4.2. A second strictly convex program reformulation of (2.7–2.8)

We now investigate another linear complementarity problem, related to (2.7–2.8), that is a useful block in setting up a fixed point iteration.

$$\begin{bmatrix} M^{(l)} & -\widetilde{\nu} & -\widetilde{n} & -\widetilde{D} \\ \widetilde{\nu}^T & 0 & 0 & 0 \\ \widetilde{n}^T & 0 & 0 & 0 \\ \widetilde{D}^T & 0 & 0 & 0 \end{bmatrix} \begin{bmatrix} v \\ c_\nu \\ c_n \\ \widetilde{\beta} \end{bmatrix} + \begin{bmatrix} -Mv^{(l)} - hk^{(l)} \\ 0 \\ \Delta \\ \tilde{E}\lambda \end{bmatrix} = \begin{bmatrix} 0 \\ 0 \\ \tilde{\rho} \\ \widetilde{\sigma} \end{bmatrix} \tag{4.27}$$

$$\begin{bmatrix} c_n \\ \widetilde{\beta} \end{bmatrix}^T \begin{bmatrix} \rho \\ \widetilde{\sigma} \end{bmatrix} = 0, \qquad \begin{bmatrix} c_n \\ \widetilde{\beta} \end{bmatrix} \geq 0, \qquad \begin{bmatrix} \rho \\ \widetilde{\sigma} \end{bmatrix} \geq 0\,. \tag{4.28}$$

Here we consider λ to be a fixed quantity, and not a variable of the problem. One can immediately see that the linear complementarity problem (4.27–4.27) represents the optimality conditions of the quadratic program

$$\begin{array}{lll} \min_v \frac{1}{2} v^T M^{(l)} v + q^{(l)^T} v & & \\ \text{subject to} \qquad n^{(j)^T} v \geq -\Delta^{(j)}, & j \in \mathcal{A} & \\ \qquad D^{(j)^T} v \geq -\lambda^{(j)} e^{(j)}, & j \in \mathcal{A} & \\ \qquad v_i^T v = 0, & i = 1, 2, \ldots, p, & \end{array} \tag{4.29}$$

where $\lambda \geq 0$ is given. In this section we will assume that $\Delta \geq 0$, and thus that (4.29) is feasible.

Since we assume that $M^{(l)}$ is positive definite, it follows that (4.29) has a unique solution $v^*(\lambda)$.

$$P_2(\lambda) = v^*(\lambda). \tag{4.30}$$

which is well defined whenever (4.21) is feasible.

Lemma 3. *Assume that (v^*, λ^*) are components of the solution of (2.7-2.8). Then the solution of (4.29) with $\lambda = \lambda^*$ is exactly v^*, or $P_2(\lambda^*) = v^*$.*

Proof. Let $\left(v^*, c_v, c_n, \tilde{\beta}, \lambda^*\right)$ be a solution of (2.7–2.8). By comparing the linear complementarity problems (2.7–2.8) and (4.27–4.28), we see that if we set $\lambda = \lambda^*$, we obtain that $\left(v^*, c_v, c_n, \tilde{\beta}\right)$ is a solution of (4.27–4.28). The conclusion follows by our previous observation that (4.27–4.28) are the optimality conditions of (4.29), and thus v^* is the unique solution of (4.29) for $\lambda = \lambda^*$. □

4.3. Features of the reformulations

Lemma 4. *Consider the quadratic program*

$$\begin{array}{rl} \min_v & \frac{1}{2} v^T Q v + q^T v \\ \textit{subject to} & A^T v \geq -\Psi \\ & B^T v = 0, \end{array} \tag{4.31}$$

where $\Psi \geq 0$ is a vector, A and B are matrices of the appropriate dimensions, and the matrix Q is symmetric positive definite, or $Q \succ 0$. Let v^* be its solution. Then $\|Q^{\frac{1}{2}} v^*\|_2 \leq \|Q^{-\frac{1}{2}} q\|_2$.

Proof. Since $v = 0$ is feasible and Q is positive definite, the quadratic program (4.31) has a solution v^*. Let $\eta \geq 0$ be the Lagrange multipliers of the inequality constraints and ζ be the Lagrange multipliers of the equality constraints. We then have the following first-order conditions:

$$Qv^* + q - A\eta - B\zeta = 0, \; A^T v^* + \Psi \geq 0, \; \left(A^T v^* + \Psi\right)^T \eta = 0, \; B^T v^* = 0.$$

Multiplying the first equation with ${v^*}^T$ to the left and using the constraints and the complementarity condition, we obtain

$$
{v^*}^T Q v^* + q^T v^* + \eta^T \Psi = 0.
$$

This, in turn, implies, since $\eta \geq 0$ and $\Psi \geq 0$, that

$$
{v^*}^T Q v^* \leq -q^T v^*,
$$

or that

$$
\| Q^{\frac{1}{2}} v^* \|_2^2 \leq -\left(Q^{-\frac{1}{2}} q \right)^T \left(Q^{\frac{1}{2}} v^* \right) \leq \| Q^{\frac{1}{2}} v^* \|_2 \| Q^{-\frac{1}{2}} q \|,
$$

where the last inequality follows from Cauchy-Schwartz. The claim follows after dividing the last inequality by $\| Q^{\frac{1}{2}} v^* \|_2$, if nonzero. □

As an immediate consequence of this lemma, which we apply to previously defined quadratic programs, we obtain the following corollaries.

Corollary 1. *Whenever* $\Gamma \geq 0$, $\Delta \geq 0$ *and* $\Upsilon = 0$, *the solution* $v^*(\Gamma)$ *of (4.21) satisfies* $\| {M^{(l)}}^{\frac{1}{2}} v^*(\Gamma) \|_2 \leq \| {M^{(l)}}^{-\frac{1}{2}} q^{(l)} \|_2$. *That is,* $\| {M^{(l)}}^{\frac{1}{2}} P_1(\Gamma) \|_2 \leq \| {M^{(l)}}^{-\frac{1}{2}} q^{(l)} \|_2$.

Corollary 2. *Whenever* $\lambda \geq 0$, $\Delta \geq 0$ *and* $\Upsilon = 0$, *the solution* $v^*(\lambda)$ *of (4.29) satisfies* $\| {M^{(l)}}^{\frac{1}{2}} v^*(\lambda) \|_2 \leq \| {M^{(l)}}^{-\frac{1}{2}} q^{(l)} \|_2$. *That is,* $\| {M^{(l)}}^{\frac{1}{2}} P_2(\lambda) \|_2 \leq \| {M^{(l)}}^{-\frac{1}{2}} q^{(l)} \|_2$.

Lemma 5. *If the friction cone of the current configuration is pointed, then the quadratic program (4.21) satisfies MFCQ.*

Proof. Assume that at some point v (4.21) does not satisfy MFCQ. Then, from (2.13) it follows that there exist the multipliers $\eta_k^{(j)} \geq 0$, $j \in \mathcal{A}$, $k = 1, 2, \ldots, m_C^{(j)}$ and $c_{\nu,i}$, $i = 1, 2, \ldots, p$, not all 0, such that

$$
0 = \sum_{j \in \mathcal{A}} \sum_{k=1}^{m_C^{(j)}} \eta_k^{(j)} \left(n^{(j)} + \mu^{(j)} d_k^{(j)} \right) + \sum_{i=1,2,\ldots,p} c_{\nu,i} \nu_i. \tag{4.32}
$$

This form is implied by the one described in (2.13), and is sufficient to prove our claim. Define now, for $j \in \mathcal{A}$,

$$
\begin{aligned}
c_n^{(j)} &= \sum_{k=1}^{m_C^{(j)}} \eta_k^{(j)} \geq 0 \\
\beta_k^{(j)} &= \mu^{(j)} \eta_k^{(j)} \geq 0, \quad k = 1, 2, \ldots, m_c^{(j)} \\
\beta^{(j)} &= \left[\beta_1^{(j)}, \beta_2^{(j)}, \ldots, \beta_{m_C^{(j)}}^{(j)} \right].
\end{aligned}
$$

One can immediately see with this definition that, for $j \in \mathcal{A}$,

$$\mu^{(j)} c_n^{(j)} = \sum_{k=1}^{m_C^{(j)}} \beta_k^{(j)} = \mu^{(j)} e^{(j)^T} \beta^{(j)} = \mu^{(j)} \|\beta^{(j)}\|_1.$$

Therefore, $c_n = \left\{c_n^{(j)}\right\}_{j\in\mathcal{A}}$, $\tilde{\beta} = \left\{\beta^{(j)}\right\}_{j\in\mathcal{A}}$ and $c_\nu = \left\{c_{\nu,i}\right\}_{i=1,2,\ldots,p}$ satisfy the inequalities defining the friction cone $FC(q)$ (2.9), are not all 0 (from our choice of η and c_ν), and from (4.32) satisfy

$$0 = \tilde{n} c_n + \tilde{D}\tilde{\beta} + \tilde{\nu} c_\nu.$$

This contradicts the assumption that the cone is pointed and hence proves the claim. □

An important consequence of MFCQ holding for (4.21) is that (4.21) is feasible for any choice of Γ, Δ and Υ [27].

4.4. Lipschitz continuity

The algorithms we consider here are fixed-point iterations, based on (4.17–4.18) and (4.27–4.28), where Γ and λ are computed based on the velocity at the previous iteration. To be able to prove our convergence results for these algorithms, we have to obtain some Lipschitz continuity results of the solution maps $P_1(\Gamma)$ and $P_2(\lambda)$ of the strictly convex associated programs (4.21) and (4.29).

Since the function $\max\{x_1, x_2, \ldots, x_n\}$ is globally Lipschitz with a Lipschitz parameter of 1 in the $\|\cdot\|_\infty$ in $\mathbb{R}^n$, it follows that the mapping defining λ^* as a function of v^* in (4.23) is globally Lipschitz with a parameter K_D that depends on the vectors $d_i^{(j)}$ defining the tangential forces at each contact.

Lemma 6. *There exists a parameter $K_D \geq 0$ such that for any two velocities v_1 and v_2,*

$$\|\Lambda(v_1) - \Lambda(v_2)\|_\infty \leq K_D \|v_1 - v_2\|_\infty.$$

Proof. Note that the definition of Λ yields for any $j \in \mathcal{A}$

$$\begin{aligned}\left|\Lambda^{(j)}(v_1) - \Lambda^{(j)}(v_2)\right| &= \left|\max_{i=1,2,\ldots,m_C^{(j)}} \left\{d_i^{(j)^T}(v_1)\right\} - \max_{i=1,2,\ldots,m_C^{(j)}} \left\{d_i^{(j)^T}(v_2)\right\}\right| \\ &\leq \max_{i=1,2,\ldots,m_C^{(j)}} |d_i^{(j)^T}(v_1 - v_2)| = \|D^{(j)^T}(v_1 - v_2)\|_\infty \\ &\leq \|D^{(j)^T}\|_\infty \|(v_1 - v_2)\|_\infty \leq \|\tilde{D}\|_\infty \|(v_1 - v_2)\|_\infty.\end{aligned} \tag{4.33}$$

for all $j \in \mathcal{A}$. The conclusion follows after taking $K_D = \|\tilde{D}\|_\infty$. □

To simplify our discussion for our next result, we denote by $\hat{\mu} = \text{diag}(\tilde{\mu})$.

Theorem 3. *(i) Let $K_\Gamma > 0$ and $K_\mu > 0$ such that the friction cone $FC(q)$ is pointed whenever $\|\hat{\mu}\|_\infty \le K_\mu$, $\forall j \in \mathcal{A}$. Then there exists $L(K_\Gamma, K_\mu)$ such that for any Γ_1 and Γ_2 such that $\|\Gamma_1\|_\infty \le K_\Gamma$ and $\|\Gamma_2\|_\infty \le K_\Gamma$ we have*

$$\|P_1(\Gamma_1) - P_1(\Gamma_2)\|_\infty \le L(K_\Gamma, K_\mu)\|\Gamma_1 - \Gamma_2\|_\infty.$$

(ii) Let $\mathcal{M}$ be a convex compact set such that $FC(q)$ is pointed whenever $\hat{\mu} \in \mathcal{M}$, and let $K_\Gamma > 0$. There exists $L(K_\Gamma, \mathcal{M})$ such that for any $\hat{\mu} \in \mathcal{M}$, Γ_1 and Γ_2 such that $\|\Gamma_1\|_\infty \le K_\Gamma$ and $\|\Gamma_2\|_\infty \le K_\Gamma$ we have

$$\|P_1(\Gamma_1) - P_1(\Gamma_2)\|_\infty \le L(K_\Gamma, \mathcal{M})\|\Gamma_1 - \Gamma_2\|_\infty.$$

Here $P_1(\Gamma) = v^*(\Gamma)$, the unique solution of the quadratic program (4.21), when it exists.

Proof of Part (i). Since the friction cone $FC(q)$ is pointed whenever $\|\hat{\mu}\|_\infty \le K_\mu$, then, from Lemma 5 the quadratic program (4.21) satisfies MFCQ whenever $\|\hat{\mu}\|_\infty \le K_\mu$. Therefore the quadratic program (4.21) is feasible for any Γ, Δ and Υ and the mapping $P_1(\Gamma)$ is well defined for any Γ. Since the matrix $M^{(l)}$ is positive definite, the strong second-order conditions required by Robinson's local Lipschitz result [27] hold. Therefore, for any Γ_0 and $\hat{\mu}_0$, satisfying $\|\hat{\mu}_0\|_\infty \le K_\mu$, there exist a parameter $L(\Gamma_0, \hat{\mu}_0)$ and neighborhoods $\mathcal{V}(\Gamma_0)$ and $\mathcal{V}(\hat{\mu}_0)$ such that $\forall \Gamma_1, \Gamma_2 \in \mathcal{V}(\Gamma_0)$ and $\forall \hat{\mu}_1, \hat{\mu}_2 \in \mathcal{V}(\hat{\mu}_0)$, we have that

$$\|v^*(\Gamma_1, \hat{\mu}_1) - v^*(\Gamma_2, \hat{\mu}_2)\|_\infty \le L(\Gamma_0, \hat{\mu}_0)\left(\|\Gamma_1 - \Gamma_2\|_\infty + \|\hat{\mu}_1 - \hat{\mu}_2\|_\infty\right).$$

Here we denote by $v^*(\Gamma, \hat{\mu})$ the solution of (4.21), to emphasize the possible dependence of the solution on the friction coefficients.

Since $v^*(\Gamma, \hat{\mu})$ is a locally Lipschitz mapping, then, when we restrict it over the compact set defined by the inequalities $\|\Gamma\|_\infty \le K_\Gamma$ and $\|\hat{\mu}\|_\infty \le K_\mu$, it becomes globally Lipschitzian. Therefore there exists $L(K_\Gamma, K_\mu)$ such that

$$\|v^*(\Gamma_1, \hat{\mu}_1) - v^*(\Gamma_2, \hat{\mu}_2)\|_\infty \le L(K_\Gamma, K_\mu)\left(\|\Gamma_1 - \Gamma_2\|_\infty + \|\hat{\mu}_1 - \hat{\mu}_2\|_\infty\right).$$

When $\hat{\mu}$ is fixed, then v^* can be considered to be a function of Γ alone. Replacing $\hat{\mu}_1 = \hat{\mu}_2 = \hat{\mu}$ in the previous equation proves part (i). □

Proof of Part (ii). As above, $v^*(\Gamma, \hat{\mu})$ is a locally Lipschitz mapping for $\|\Gamma\|_\infty \le K_\Gamma$ and $\hat{\mu} \in \mathcal{M}$. Therefore $v^*(\Gamma, \hat{\mu})$ is a globally Lipschitz mapping over $\left\{\Gamma \,|\, \|\Gamma\|_\infty \le K_\Gamma\right\} \times \mathcal{M}$. Therefore there exists $L(K_\Gamma, \mathcal{M})$ such that

$$\|v^*(\Gamma_1, \hat{\mu}_1) - v^*(\Gamma_2, \hat{\mu}_2)\|_\infty \le L(K_\Gamma, \mathcal{M})\left(\|\Gamma_1 - \Gamma_2\|_\infty + \|\hat{\mu}_1 - \hat{\mu}_2\|_\infty\right)$$

whenever $\|\Gamma_1\|_\infty \le K_\Gamma$, $\|\Gamma_2\|_\infty \le K_\Gamma$ and $\hat{\mu}_1, \hat{\mu}_2 \in \mathcal{M}$. The conclusion of part ii) follows by taking $\hat{\mu}_1 = \hat{\mu}_2 = \hat{\mu}$. □

The Lipschitz continuity of $P_2(\lambda)$ is considerably easier to demonstrate, because the constraints of (4.29) are not affected by the friction coefficient, so we do not have to ensure uniformity of the Lipschitz parameter with respect to the friction coefficient.

Theorem 4. *Assume that $\Delta \geq 0$. There exists a parameter $L_2 \geq 0$ such that $\| P_2(\lambda_1) - P_2(\lambda_2)\|_\infty \leq L_2 \|\lambda_1 - \lambda_2\|_\infty$, $\forall \lambda_1,\ \lambda_2 \in I\!R^{\,\mathrm{card}\{\mathcal{A}\}}$, $\lambda_1,\ \lambda_2 \geq 0$.*

Proof. Since $\Delta \geq 0$, it follows that (4.29) is feasible and its solution mapping $P_2(\lambda)$ is well defined for $\lambda \geq 0$. The conclusion of the statement is an immediate consequence of Theorem 1. The Theorem applies since the quadratic program (4.29) is strictly convex, it does not depend on $\tilde{\mu}$, and its parameter λ affects only the right-hand side. □

4.5. Fixed-point reformulation and contraction property

The fundamental result of this section is based on analyzing the properties of a series of aggregate maps. Recall that, following the definition of the mixed linear complementarity problem (2.7–2.8), $\tilde{\mu}$ is a diagonal matrix whose entries are the friction coefficients at the individual contacts.

4.5.1. Fixed point formulation based on P_1. Using (4.22), we define the first aggregate map by

$$\chi_1(v) = P_1(\tilde{\mu}\Lambda(v)). \tag{4.34}$$

Lemma 7. *Assume that $\Upsilon = 0$. The quantity v^* is the velocity component of a solution of the mixed linear complementarity problem (2.7–2.8) if and only if it is a fixed point of $\chi_1(v)$.*

Proof. Let $\left(v^*, c_\nu, c_n, \tilde{\beta}, \lambda\right)$ be a solution of (2.7–2.8). It is then immediate that $\left(v^*, c_\nu, c_n, \tilde{\beta}, \Lambda(v)\right)$ is also a solution of the problem (2.7–2.8). In effect, the only change in the new solution is that $\lambda^{(j)}$ corresponding to a contact that satisfies $D^{(j)^T} v^* = 0$ is set to 0. Therefore, after comparing (2.7–2.8) and (4.17–4.18) we see that $\left(v^*, c_\nu, c_n, \tilde{\beta}, \Lambda(v^*)\right)$ is a solution of (4.17–4.18) with $\Gamma = \tilde{\mu}\Lambda(v^*)$. Using Lemma 2, Lemma 1, the definition of the mapping P_1 (4.22), and Theorem 2, we get that $v^* = P_1(\tilde{\mu}\Lambda(v^*))$, which shows that v^* is a fixed point of the mapping χ_1.

Conversely, let v^* be a fixed point of χ_1, or $v^* = P_1(\tilde{\mu}\Lambda(v^*))$. Since P_1 is the solution mapping associated with the strictly convex quadratic program (4.21) we obtain from Theorem 2 that $(v^*, \Lambda(v^*))$ is a solution of (4.20) for the choice of $\Gamma = \tilde{\mu}\Lambda(v^*)$. In turn, Lemma 2 implies that, for appropriate multipliers, $(v^*, c_\nu, c_n, \tilde{\beta}, \Lambda(v^*))$ is a solution of (4.17–4.18) for $\Gamma = \tilde{\mu}\Lambda(v^*)$. Finally Lemma 1 shows that $(v^*, c_\nu, c_n, \tilde{\beta}, \Lambda(v^*))$ is a solution of (2.7–2.8) and proves the rest of the claim. □

The following results require upper bound conditions on the friction coefficients. In order to invoke the results from Section 4.4, recall that $\tilde{\mu}$ is a diagonal matrix, whose diagonal is the vector $\hat{\mu}$ and that the following equation holds

$$\|\tilde{\mu}\|_\infty = \|\hat{\mu}\|_\infty.$$

Lemma 8. *Assume that, for $\tilde{\mu} = 0$, the friction cone $FC(q)$ is pointed. Let S be a compact set in $I\!R^n$. Then there exists $\mu^\circ > 0$ such that whenever $\|\tilde{\mu}\|_\infty \leq \mu^\circ$, we have that, for any $v_1, v_2 \in S$ the mapping $\chi_1(v)$ is well defined and satisfies*

$$\|\chi_1(v_1) - \chi_1(v_2)\|_\infty \leq \frac{1}{2}\|v_1 - v_2\|_\infty.$$

Proof. Define

$$\mu^* = \frac{1}{2}\max\left\{\mu \geq 0 | FC(q) \text{ is a pointed cone whenever } \|\tilde{\mu}\|_\infty < \mu\right\}.$$

Since $FC(q)$ is polyhedral and pointed when $\tilde{\mu} = 0$, it follows that $\mu^* > 0$. Whenever $\|\tilde{\mu}\|_\infty < 2\mu^*$, we have that (4.21) satisfies MFCQ from Lemma 5 since the friction cone is pointed.

Thus whenever $\|\tilde{\mu}\|_\infty \leq \mu^*$, we have that P_1, the solution mapping, is well defined which, in turn, implies that χ_1 is well defined. Choose $K_\mu = \mu^*$ and

$$K_\Gamma = \max_{v \in S}\left\{\mu^*\|\Lambda(v)\|_\infty\right\}$$

$$\mu^\circ = \min\left\{\mu^*, \frac{1}{2L(K_\Gamma, K_\mu)K_D}\right\} > 0,$$

where $L(K_\Gamma, K_\mu)$ is the Lipschitz parameter of P_1 under the conditions specified in Theorem 3(i) and K_D is the Lipschitz parameter in Lemma 6. Pick any two points $v_1, v_2 \in S$ and $\tilde{\mu}$ such that $\|\tilde{\mu}\|_\infty \leq \mu^\circ$. Then from Lemma 6 we have that

$$\|\Lambda(v_1) - \Lambda(v_2)\|_\infty \leq K_D\|v_1 - v_2\|_\infty.$$

In turn, this implies that

$$\|\tilde{\mu}\Lambda(v_1) - \tilde{\mu}\Lambda(v_2)\|_\infty \leq \|\tilde{\mu}\|_\infty\|\Lambda(v_1) - \Lambda(v_2)\|_\infty \leq \|\tilde{\mu}\|_\infty K_D\|v_1 - v_2\|_\infty.$$

Finally we use Theorem 3(i), which applies because of our choice of K_Γ. Since $\|\tilde{\mu}\Lambda(v_1)\|_\infty \leq K_\Gamma$ and $\|\tilde{\mu}\Lambda(v_2)\|_\infty \leq K_\Gamma$ and since, from our choice of μ°, the friction cone is uniformly pointed whenever $\tilde{\mu} \leq \mu^\circ$, we have that

$$\|\chi(v_1) - \chi(v_2)\| = \|v^*(\tilde{\mu}\Lambda(v_1)) - v^*(\tilde{\mu}\Lambda(v_2))\|_\infty \leq L(K_\Gamma, K_\mu)\|\tilde{\mu}\|_\infty K_D\|v_1 - v_2\|_\infty.$$

With the choice of μ° as above, we immediately obtain that for any $v_1, v_2 \in S$, whenever $\|\tilde{\mu}\| \leq \mu^\circ$,

$$\|\chi_1(v_1) - \chi_1(v_2)\|_\infty \leq \frac{1}{2}\|v_1 - v_2\|_\infty,$$

which completes the proof. □

We can now state the main result of our development for this map.

Theorem 5. *Assume that, for $\tilde{\mu} = 0$, the friction cone $FC(q)$ is pointed and that $\Delta \geq 0$ and $\Upsilon = 0$. Consider the set $S = \left\{v \,\middle|\, \|M^{(l)^{\frac{1}{2}}}v\|_2 \leq \|M^{(l)^{-\frac{1}{2}}}q^{(l)}\|_2\right\}$. Then $\chi_1(S) \subseteq S$ and there exists a $\mu^\circ > 0$ such that, whenever $\|\tilde{\mu}\|_\infty \leq \mu^\circ$ we have that χ_1 is a contraction over S of parameter $\frac{1}{2}$ in the infinity norm.*

Proof. Take a vector $v \in S$ and construct $\Gamma = \tilde{\mu}\Lambda(v)$. From (4.23) and the fact that the vectors defining the polyhedral approximation to the friction cone form a balanced set, we obtain that $\Gamma \geq 0$. From (4.34) we have that $\chi_1(v) = P_1(\Gamma)$, the solution of (4.21). From Corollary 1, it immediately follows that $P_1(\Gamma)$, and thus $\chi_1(v)$ satisfies the inequality that defines S, which implies that $\chi_1(S) \subset S$. Using Lemma 8 we obtain the conclusion of the proof. □

From here we get the following important corollary.

Corollary 3. *Under the conditions of Theorem 5 (sufficiently small friction coefficient), the mixed linear complementarity problem (2.7–2.8) has a unique velocity solution. The solution can be found by a fixed point iteration of the mapping $\chi_1(v)$ that converges at least linearly to the solution.*

Proof. The conclusion is immediate from the properties of contractions, Theorem 5, and Lemma 7. □

We now apply the concepts developed in this section to the example from Section 3. Using our observations concerning pointed friction cones in Section 2.3.1, we see that the configuration in the example can be disassembled (a sufficiently large upwards impulse induces simultaneous break of all contacts) and thus has a pointed friction cone when $\tilde{\mu} = 0$. Therefore, Theorem 5 applies to show that, for sufficiently small friction coefficients, the example has a unique velocity solution, although the solution set of (2.7–2.8) is nonconvex. Hence our fixed-point iteration converges for some configurations to the velocity solution while solving convex subproblems, despite the fact that the solution set is nonconvex.

4.5.2. Fixed point iteration based on P_1 and P_2. In this section, we assume throughout that $\Delta \geq 0$ and $\Upsilon = 0$. The second mapping under consideration is

$$\chi_2(v) = P_2 \circ \Lambda \circ P_1 \circ (\tilde{\mu}\Lambda(v)) . \tag{4.35}$$

Lemma 9. *If v^* is a velocity solution of (2.7–2.8) then v^* is a fixed point of $\chi_2(v)$.*

Proof. This is an immediate consequence of Lemma 1, Lemma 2, Theorem 2, and Lemma 3. □

Theorem 6. *(i) Consider the set $S = \left\{ v \,\middle|\, \|M^{(l)^{\frac{1}{2}}} v\|_2 \leq \|M^{(l)^{-\frac{1}{2}}} q^{(l)}\|_2 \right\}$. Then $\chi_2(S) \subseteq S$.*

(ii) Assume that, for $\tilde{\mu} = 0$, the friction cone $FC(q)$ is pointed. Then there exists $\mu^\circ > 0$ such that, whenever $\|\tilde{\mu}\|_\infty \leq \mu^\circ$, the mapping $\chi_2(v)$ is a contraction over S in the $\|\cdot\|_\infty$ norm, with parameter $\frac{1}{2}$.

Proof of Part (i). Take a vector $v \in S$ and define $v_1 = \chi_2(v)$ and $\lambda = \Lambda \circ P_1 \circ (\tilde{\mu}\Lambda(v))$. From the definition of the mapping (4.35) we get that $v_1 = P_2(\lambda)$. From the definition (4.23) of the mapping Λ we get that $\lambda \geq 0$. Finally, using Corollary 2, we obtain that $v_1 \in S$, which proves the claim of part (i). □

Proof of Part (ii). Define

$$\mu^* = \frac{1}{2} \max \{\mu \geq 0 | FC(q) \text{ is a pointed cone whenever } \|\tilde{\mu}\| \leq \mu\}.$$

Since $FC(q)$ is polyhedral and pointed when $\tilde{\mu} = 0$, it follows that $\mu^* > 0$. Choose now $K_\mu = \mu^*$

$$K_\Gamma = \max_{v \in S} \left\{ \mu^* \|\Lambda(v)\|_\infty \right\}$$

$$\mu^\circ = \min \left\{ \mu^*, \frac{1}{2L(K_\Gamma, K_\mu) L_2 K_D^2} \right\} > 0,$$

where $L(K_\Gamma, K_\mu)$ is Lipschitz parameter of mapping P_1 from Theorem 3(i), L_2 is the global Lipschitz parameter of the mapping P_2 from Theorem 4, and K_D is the Lipschitz parameter in Lemma 6. Pick any two points $v_1, v_2 \in S$ and $\tilde{\mu}$ such that $\|\tilde{\mu}\|_\infty \leq \mu^\circ$. Then

$$\begin{aligned}
\|\chi_2(v_1) - \chi_2(v_2)\|_\infty &= \|P_2 \circ \Lambda \circ P_1 \circ (\tilde{\mu}\Lambda(v_1)) - P_2 \circ \Lambda \circ P_1 \circ (\tilde{\mu}\Lambda(v_2))\|_\infty \\
&\leq L_2 \|\Lambda \circ P_1 \circ (\tilde{\mu}\Lambda(v_1)) - \Lambda \circ P_1 \circ (\tilde{\mu}\Lambda(v_2))\|_\infty \\
&\leq L_2 K_D \|P_1 \circ (\tilde{\mu}\Lambda(v_1)) - P_1 \circ (\tilde{\mu}\Lambda(v_2))\|_\infty \\
&\leq L_2 K_D L(K_\Gamma, K_\mu) \|\tilde{\mu} (\Lambda(v_1) - \Lambda(v_2))\|_\infty \\
&\leq L_2 K_D L(K_\Gamma, K_\mu) \|\tilde{\mu}\|_\infty \| (\Lambda(v_1) - \Lambda(v_2))\|_\infty \\
&\leq \mu^\circ L_2 L(K_\Gamma, K_\mu) K_D^2 \|v_1 - v_2\|_\infty \leq \tfrac{1}{2} \|v_1 - v_2\|_\infty.
\end{aligned} \tag{4.36}$$

At the fourth inequality we have used Theorem 3(i), which applies because $v_1, v_2 \in S$ implies that $\|\tilde{\mu}\Lambda(v_1)\|_\infty \leq K_\Gamma$ and $\|\tilde{\mu}\Lambda(v_2)\|_\infty \leq K_\Gamma$ from our choice of K_Γ and our choice of K_μ and μ° ensures that the friction cone is uniformly pointed whenever $\|\tilde{\mu}\|_\infty \leq \mu^\circ$. This proves that for the parametric choices outlined above, the mapping χ_2 is a contraction mapping with parameter $\frac{1}{2}$. □

The observation must be made here that since P_2 produces a velocity component that is independent of the friction, it seems reasonable that unless we have prior knowledge of λ^*, we would need some way of estimating this parameter. Fortunately, this is a byproduct of the mapping P_1, which explains the convergence result above.

For efficiency reasons, especially in real time applications, one may wish to stop a fixed point iteration algorithm significantly before its convergence. In that case one may consider using as an approximation to the solution velocity just the first iteration of one of the fixed-point methods. The following result estimates the error in velocity when doing one such operation.

Theorem 7. *Let $\mathcal{M}$ be a convex compact set such that $FC(q)$ is a pointed cone whenever $\hat{\mu} = \operatorname{diag}(\tilde{\mu}) \in \mathcal{M}$. Let $S = \left\{ v \middle| \|M^{(l)^{\frac{1}{2}}} v\|_2 \leq \|M^{(l)^{-\frac{1}{2}}} q^{(l)}\|_2 \right\}$ and $K_\Gamma = \max_{v \in S} \left\{ \mu^* \|\Lambda(v)\|_\infty \right\}$. Then for any velocity solution v^* of (2.7–2.8) the following inequalities hold:*

(i) $\|v^* - \chi_1(0)\|_\infty \leq L(K_\Gamma, \mathcal{M})\|\tilde{\mu}\Lambda(v^*)\|_\infty$,
(ii) $\|v^* - \chi_2(0)\|_\infty \leq L_2 K_D L(K_\Gamma, \mathcal{M})\|\tilde{\mu}\Lambda(v^*)\|_\infty$.

Here L_2 and K_D are the Lipschitz parameters of the maps P_2 and Λ, whereas $L(K_\Gamma, \mathcal{M})$ is the parameter from Theorem 3 (ii).

Proof. We prove only the case (ii), the proof of the case (i) being almost identical. Using Lemma 9, we obtain that $v^* = \chi_2(v^*) = P_2 \circ \Lambda \circ P_1\,(\tilde{\mu}\Lambda(v^*))$. Therefore

$$\begin{aligned}\|v^* - \chi_2(0)\|_\infty &= \|P_2 \circ \Lambda \circ P_1\,(\tilde{\mu}\Lambda(v^*)) - P_2 \circ \Lambda \circ P_1\,(\tilde{\mu}\Lambda(0))\,\|_\infty \\ &\leq L_2 K_D \|P_1\,(\tilde{\mu}\Lambda(v^*)) - P_1(0)\|_\infty \leq L_2 K_D L(K_\Gamma, \mathcal{M})\|\tilde{\mu}\Lambda(v^*)\|_\infty,\end{aligned}$$

where the last inequality follows from Theorem 3 (ii). □

The last result shows that one step of the fixed-point iteration based on either the map χ_1 or the map χ_2 (which solved two convex quadratic programs) results in an approximation to v^* whose error is proportional to $\|\tilde{\mu}\Lambda(v^*)\|_\infty$. This approximation is very good when either the friction coefficient is small or when the friction coefficient is large but the tangential velocity is small. *In particular,* configurations that have a no slip solution are computed exactly by this method.

5. Fixed-point iteration algorithms

We now describe fixed-point iteration algorithms in terms of the quadratic programs or, equivalently, linear complementarity programs introduced in the preceding sections. To simplify the discussion, we assign acronyms to all algorithms. We call LCP0 the resolution of (2.7–2.8) directly by Lemke's method.

5.1. Fixed-point iteration algorithm based on χ_1

In terms of χ_1, the fixed-point algorithm is expressed simply as $v^*(0) = 0$, $v^*(\kappa+1) = \chi_1(v^*(\kappa))$. Using the definition of χ_1, (4.34), we can express the fixed point iteration in terms of certain convex quadratic programs.

1. Set $\Gamma(0) = 0$, $\kappa = 0$, $v^*(0) = 0$.
2. Set $v^*(\kappa+1) = P_1(\Gamma(\kappa))$: Solve the mixed linear complementarity problem (4.17–4.18) for $\Gamma = \Gamma(\kappa)$ (or, equivalently, the quadratic program (4.21)), and find the new velocity $v^*(\kappa+1) = v^*(\Gamma(\kappa))$.
3. Set $\lambda(\kappa+1) = \Lambda(v^*(\kappa+1))$ from (4.23):
$$\lambda^{(j)}(\kappa+1) = \max_{i=1,2,\ldots,m_C^{(j)}} \left\{ d_i^{(j)^T} v^*(\kappa+1) \right\}, \quad j \in \mathcal{A}. \tag{5.37}$$
4. Set $\Gamma(\kappa+1) = \tilde{\mu}\lambda(\kappa+1)$. Recall from the discussion following the definition of the mixed linear complementarity problem (2.7–2.8) that $\tilde{\mu}$ is a diagonal matrix whose entries are the friction coefficients of the individual contacts. From the assumption that the tangential force description is balanced, we clearly have that $\Gamma(\kappa) \geq 0$, $\forall\kappa$.

5. Check for convergence. If the convergence test is not satisfied, set $\kappa = \kappa + 1$, and return to Step 2.

To simplify further discussion, we call this algorithm LCP1.

From Corollary 3 we obtain that for sufficiently small but nonzero friction this algorithm converges to the unique velocity solution of the mixed linear complementarity problem (2.7–2.8). This convergence is achieved globally (always initializing the algorithm with $v = 0$), with a fixed linear rate, while solving (at Step 2 of the algorithm) only convex subproblems (linear complementarity problems with positive semidefinite matrices).

5.2. Fixed point iteration algorithm based on χ_2

Similarly, for χ_2 we can define the fixed-point iteration algorithm $v^*(0) = 0$, $v^*(\kappa+1) = v^*(\kappa)$. Using the definition of χ_2 (4.35), we can express the steps of the algorithm in terms of convex quadratic programs.

1. Set $\Gamma(0) = 0$, $\kappa = 0$, $v^*(0) = 0$.
2. Set $\hat{v}^*(\kappa+1) = P_1(\Gamma(\kappa))$: Solve the mixed linear complementarity problem (4.17–4.18) for $\Gamma = \Gamma(\kappa)$ (or, equivalently, the quadratic program (4.21)), and find the new velocity $\hat{v}^*(\kappa+1) = v^*(\Gamma(\kappa))$.
3. Set $\hat{\lambda}(\kappa+1) = \Lambda(\hat{v}^*(\kappa+1))$ from (4.23):

$$\hat{\lambda}^{(j)}(\kappa+1) = \max_{i=1,2,\dots,m_C^{(j)}} \left\{ d_i^{(j)^T} \hat{v}^*(\kappa+1) \right\}, \quad j \in \mathcal{A}. \tag{5.38}$$

4. Set $v^*(\kappa+1) = P_2(\hat{\lambda}(\kappa+1))$: Solve the mixed linear complementarity problem (4.17–4.18) for $\lambda = \hat{\lambda}(\kappa+1))$ (or, equivalently, the quadratic program (4.29)), and find the new velocity $v^*(\kappa+1) = v^*(\hat{\lambda}(\kappa+1))$.
5. Set $\lambda(\kappa+1) = \Lambda(v^*(\kappa+1))$ from (4.23):

$$\lambda^{(j)}(\kappa+1) = \max_{i=1,2,\dots,m_C^{(j)}} \left\{ d_i^{(j)^T} v^*(\kappa+1) \right\}, \quad j \in \mathcal{A}. \tag{5.39}$$

6. Set $\Gamma(\kappa+1) = \tilde{\mu}\lambda(\kappa+1)$. Once again we clearly have that $\Gamma(\kappa) \geq 0$, $\forall\kappa$.
7. Check for convergence. If convergence test is not satisfied, set $\kappa = \kappa+1$, and return to Step 2.

We call this algorithm LCP2.

From Theorem 6 and Lemma 9 we obtain that for sufficiently small but nonzero friction this algorithm converges to the unique velocity solution of the mixed linear complementarity problem (2.7–2.8). This convergence is achieved globally (always initializing the algorithm with $v = 0$), with a fixed linear rate, while solving (at Step 2 of the algorithm) only convex subproblems (linear complementarity problems with positive semidefinite matrices).

An important issue is to determine when or if algorithm LCP1 is preferable to algorithm LCP2. It seems possible that, because of the extra step, algorithm LCP2 takes more work for a comparable rate of convergence. Algorithm LCP2 has one important advantage, however, for real-time simulation. In many real-time applications it may be impossible to solve the target problem in the time allocated for the computation. In that case, it is important for the algorithm to provide partial information that satisfies as many of the simulation constraints as possible. In that sense, one can immediately show that any iteration of LCP2 satisfies the linearized geometrical constraints exactly, and it provides a dissipative impulse that lives inside the friction cone. This is markedly different from LCP1, for which a partial iteration may decide that a contact must take off although the contact is dynamically active (it exhibits a nonzero contact impulse). Since most users of multibody dynamics software packages are likely to consider satisfaction of geometrical constraints more important than that of dynamical constraints, because of the immediately visible error in the first case, this may make an important difference in practical applications.

This observation also indicates that one can use as a cheaper alternative to LCP0, LCP1,or LCP2 an algorithm that uses the map χ_1 and, respectively, the map χ_2, or, equivalently, algorithm LCP1 and, respectively, the algorithm LCP2 for exactly one iteration. We call LCP3 an algorithm that uses only one iteration of LCP1. From Theorem 7 we see that the error that we need to assume in using LCP3 is of the order of $\|\tilde{\mu}\Lambda(v^*)\|$, where v^* is an exact solution of (2.7–2.8). Therefore, if the friction coefficient is small or if the friction coefficient is large but the tangential velocity λ is small, LCP3 provides a good approximation of v^*.

A similar algorithm can be defined by using LCP2 for only one iteration and, from Theorem 7, it follows that it will have the same property. Also, as argued above, such an algorithm will satisfy the geometrical constraints exactly, and it will be interesting from the perspective of real-time simulations. The difficulty is that for χ_2 we do not have the equivalent of Lemma 7, since in effect, when using the mapping P_2, we are not only perturbing a constraint, we are ignoring one (the conic constraint). It is therefore not immediate how to obtain aposteriori estimates for $\|\chi_2(0) - v^*\|$ for purposes of numerical comparison, other than computing v^*. For numerical validation, we will therefore use only LCP3.

5.3. Numerical results

We have implemented the two algorithms inside a Matlab simulation environment for rigid multibody dynamics with contact and friction. In all cases, we have simulated the cannonball arrangement in two dimensions with a variable number of disks of radius 3. There are n bodies placed on the bottom plank, all in linear contact, then $n-1$ bodies on top of these, and so forth. The time step was 0.05. The friction coefficient was 0.05, unless mentioned otherwise. All collisions are plastic. For LCP0 we used Lemke's method as implemented by PATH [14, 23]. For solving the quadratic programs in methods LCP1, LCP2, and LCP3 we also used PATH with the problems transformed in their linear complementarity form.

We ran the following examples:

1. Starting from rest, 21 disks in the cannonball arrangement (6 disks on the bottom). We compare LCP1, LCP2, LCP3, and LCP0 in Figure 2. LCP1 and LCP2, the iterative methods based on χ_1 and, respectively, χ_2, were run until $\|v^*(\kappa) - v^*(\kappa-1)\| \leq$

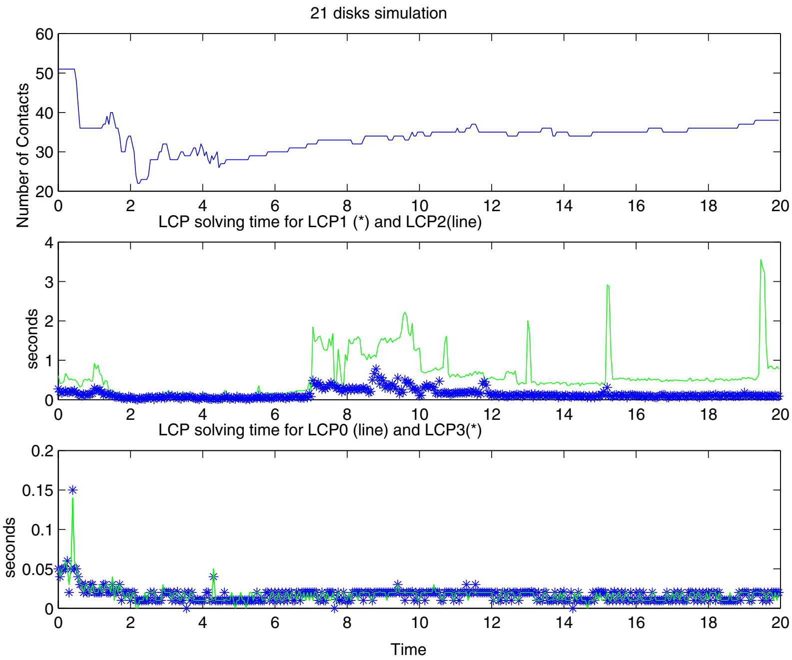

Fig. 2. Comparison of a 2D simulation with 21 bodies

$1e-5$. In the first graph we display the number of active contacts. The size of the linear complementarity problem to be solved by LCP0 is four times the number of contacts (since we pivot out the mass matrix first in (2.7–2.8) and we have no joint constraints). In the second graph we see the number of seconds spent solving LCPs by LCP1 (stars) and LCP2 (line). In the third graph we see the number of seconds spent in solving LCPs by LCP3 (stars) and LCP0 (line).

2. Starting from rest, 136 disks in the cannonball arrangement (16 disks on the bottom) with friction coefficient $\mu = 0.2$. Here LCP0, LCP1, and LCP2 failed to find a solution, so the results are plotted only for LCP3 in Figure 3: the number of contacts at various stages of the simulation and the amount of time spent solving LCPs per time step by LCP3.
3. A comparison between LCP3 and LCP0 running times for 210 disks (20 on the bottom), for the first step of the simulation. The results are displayed in Table 1 for several values of the friction coefficients. The error is the discrepancy in the linearization of the noninterpenetration constraint of the solution of (4.19), when inserted in (2.7–2.8) (since all the other constraints are the same). Through Lemma 1, the velocity solution of (4.19) coincides with the solution of (4.21), which, for $\Gamma = 0$ is the one used in $\chi_1(0)$ and thus LCP3.
4. To verify whether LCP3 will produce realistic results, we have simulated a well-known effect from granular flow: the Brazil Nut effect [28] In this simulation, it is expected that one large particle will raise to the top when shaken with smaller

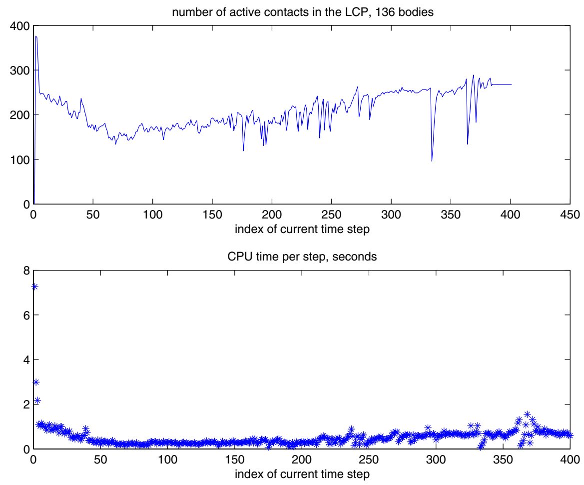

Fig. 3. Results of a 2D simulation with 136 bodies

Table 1. Comparison between the LCP0 algorithm and LCP3 for the 210 bodies example

μ	LCP0 CPU	LCP 3 CPU	LCP 3 Residual Error
0.1	29.76	34.42	0.06
0.2	MAX ITER	36.28	0.12
0.4	MAX ITER	24.03	0.07
0.6	MAX ITER	20.40	1e-8
0.8	MAX ITER	14.52	8e-11

particles. In our case, there is one large particle of radius 5 together with 269 small particles of radius 1.5. The shake is modeled by a sliding bottom bar that moves vertically. The algorithm used for simulation is LCP3 with linearization of the constraint at a fixed timestep of 100ms which is proven to achieve constraint stabilization for plastic collisions [4]. Here we have used a Newton collision restitution rule (for which we did not prove constraint stabilization), that is adapted for fixed time-step simulation [1]. The approximation Theorem 7 can be easily extended for the scheme we used in this simulation. We have used a friction coefficient of 0.5 and a restitution coefficient of 0.5.

From the above mentioned figures and table we extract the following conclusions.

1. For a small number of bodies the Lemke solver LCP0 is very efficient, more so than LCP1 and LCP2, though not more efficient than LCP3. The situation for the algorithms other than LCP0 can be considerably improved by applying specialized convex quadratic program solvers. For example, PATH uses LU factorization whereas convex QP approaches can be solved using Choleski factorizations, which would result, in a factor of 2 speed-up. Specialized techniques for convex QP approaches will be discussed in future research.
2. Both LCP1 and LCP2 have converged for 21 disks and $\mu = 0.05$. We have not apriorily determined whether the value of the friction coefficient lies within the range of

friction coefficients for which our theory predicts convergence. Nevertheless, as in most other works dealing with fixed point iterations at small friction coefficients [10, 15, 17, 24, 25], we consider this behavior to be a validation of our theoretical results.

3. Other techniques (even if approximate) are essential for larger problems because, for 136 bodies, all solvers except LCP3 (the heuristic solver) failed on the problem (here PATH failed with a maximum number of iterations message). The guarantee that LCP0 has a solution does not in itself guarantee that the solution can be found in a convenient amount of time, especially given the nonconvexity of the solution set, as illustrated by the example in Section 3. In such situations and given the real-time constraint, users may have to accept approximate but fast solutions, like the ones provided by LCP3, which are at least valid in some fairly common cases.
4. We can also see that, in some cases, LCP1, LCP2, and LCP3 do work faster than LCP0, especially at high friction, near an equilibrium solution. This can be inferred from Table 1; the P_1 part of the LCP3 step is also common for the LCP1 and LCP2 steps, since it shows that LCP1 and LCP2 would have converged for a fairly small convergence tolerance. For this particular case (at all contacts we have very slow sliding) we can see that LCP3 gives a very effective approximation of the solution at a relatively small cost.
5. When using LCP3 to simulate the Brazil Nut effect, we have obtained that the large disk migrates to the top in about 50 shakes. This is in the same range as the number of shakes obtained by Monte-Carlo simulation where the shake is simulated by a heating-cooling schedule with periodic horizontal boundary conditions [28] (in our case we have hard vertical walls). Therefore, at least for this case, the convex relaxation algorithm LCP3 produces realistic results. Four frames of the simulation are presented in Figure 4.

6. Conclusions

We consider the issue of solving the mixed linear complementarity problem that appears when designing time-stepping methods for multi-rigid-body dynamics with contact and friction.

Here we discuss the impulse-velocity approach introduced in [30, 6], that, for large friction, circumvents the problem of lack of solutions for certain rigid-body dynamics problems with contact and Coulomb friction. In this work we are interested in solving efficiently the linear complementarity problem at least for sufficiently small but nonzero friction coefficients.

We show that even simple problems such as the example presented in Section 3 may have a nonconvex solution set at rest, for arbitrarily small but nonzero friction. In effect, simple examples can be constructed based on this one where the number of solution facets grows exponentially with the size of the problem. Problems of this type may be difficult to solve.

We show that for sufficiently small friction, however, a certain fixed-point iteration converges globally and linearly to the velocity solution while solving convex subproblems, provided that the friction cone is pointed at $\tilde{\mu} = 0$, or, equivalently, that the configuration is disassemblable [2]. Fixed-point iterations have been used in the past to

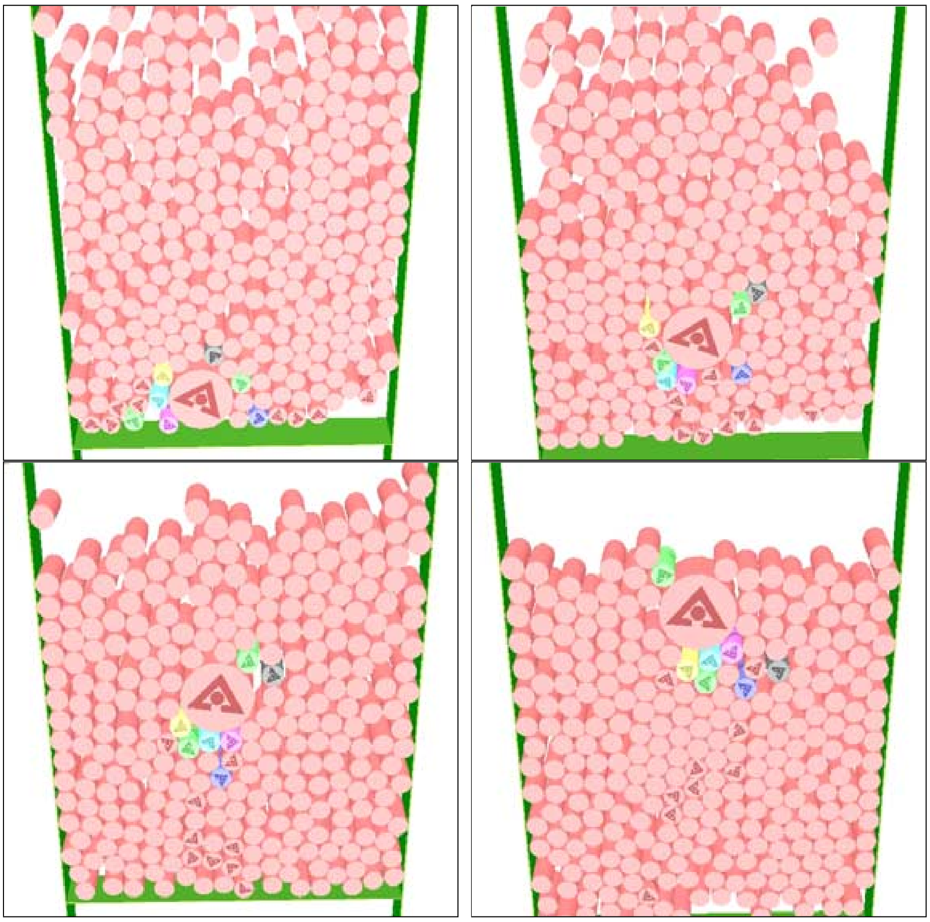

Fig. 4. Four frames of a two-dimensional Brazil nut effect simulation

solve elastostatic friction problems for small friction coefficients [10, 15, 17, 24, 25], when the force component of the solution is unique. Our method is an improvement over previous approaches in that we obtain convergence even for configurations for which the impulse or force part of the solution is not unique. In particular, even problems that have an overall nonconvex solution set like the example in Section 3 (but a unique velocity solution) can be solved by our fixed-point iteration.

It is true that, for small friction, the classical acceleration force model may have a solution and the development that treats the problem in impulse–velocity coordinates may not be necessary to get a consistent framework [16, 31]. However, if the friction is treated implicitly in mixed explicit-implicit Euler step, then one would have to solve at every step the linear complementarity problem (2.7–2.8) [7]. The implicit treatment of friction (in the sense that dissipation is enforced based on the velocity at the end of the interval) is useful because of the good energy properties [7, 6]. Therefore, the approach

(2.7–2.8) is relevant even when the configuration is consistent in a classical sense but the discrete scheme needs to preserve the energy properties of the continuous model.

We also demonstrate that efficient approximations of the linear complementarity problem (2.7–2.8) can be constructed by using only one or two convex linear complementarity problems (or, equivalently, one or two convex quadratic programs) per step. These approximations have very low error when either the friction or the tangential velocity at the contact is small, and can be seen as one step of our fixed point iteration algorithms. We demonstrated that for more than 100 bodies in two dimensions this method is much faster than solving the linear complementarity problem that may have a nonconvex solution set. In addition, the approximation satisfies many of the constraints of the simulation, and can be shown to dissipate energy, for zero external force. Such approximations may prove very important for real-time simulations where the users may be unwilling to let costly algorithms run to completion and where a coarse approximation that is physically meaningful may be sufficient. We have demonstrated that this approximation can be used to realistically simulate the Brazil nut effect [28].

Acknowledgements. Thanks to Todd Munson and Mike Ferris for providing and supporting PATH [14] and [23]. We also thank the anonymous referees for the comments that have significantly improved the paper. This work was supported by the National Science Foundation, through the award DMS-9973071, as well as the Mathematical, Information, and Computational Sciences Division subprogram of the Office of Advanced Scientific Computing, U.S. Department of Energy, under Contract W-31-109-Eng-38 (MA).

References

1. Anitescu, M.: A fixed time-step approach for multi-body dynamics with contact and friction. Preprint ANL/MCS-P1034-0303, Mathematics and Computer Science Division, Argonne National Laboratory, Argonne, Illinois, 2003
2. Anitescu, M., Cremer, J.F., Potra, F.A.: Formulating 3d contact dynamics problems. Mech. Struct. Mach. **24**(4), 405–437 (1996)
3. Anitescu, M., Cremer, J.F., Potra, J.A.: On the existence of solutions to complementarity formulations of contact problems with friction. In: Complementarity and Variational Problems: State of the Art, M.C. Ferris, J.-S. Pang (eds.), Philadelphia, SIAM Publications, 1997, pp. 12–21
4. Anitescu, M., Hart, G.D.: A constraint-stabilized time-stepping approach for rigid multibody dynamics with joints, contact and friction. Preprint ANL/MCS-1002-1002, Mathematics and Computer Science Division, Argonne National Laboratory, Argonne, Illinois, 2002
5. Anitescu, M., Lesaja, G., Potra, F.A.: Equivalence between different formulations of the linear complementarity problems. Optim. Methods Softw. **7**(3–4), 265–290 (1997)
6. Anitescu, M., Potra, F.A.: Formulating dynamic multi-rigid-body contact problems with friction as solvable linear complementarity problems. Nonl. Dyn. **14**, 231–247 (1997)
7. Anitescu, M., Potra, F.A.: Time-stepping schemes for stiff multi-rigid-body dynamics with contact and friction. Int. J. Numer. Methods Eng. **55**(7), 753–784 (2002)
8. Anitescu, M., Potra, F.A., Stewart, D.: Time-stepping for three-dimensional rigid-body dynamics. Comput. Methods Appl. Mech. Eng. **177**, 183–197 (1999)
9. Ascher, U.M., Petzold, L.R.: Computer methods for ordinary differential equations and differential-algebraic equations. Social Industrial and Applied Mathematics, Philadelphia, PA, 1998
10. Bisegna, P., Lebon, F., Maceri, F.: Dpana: A convergent block-relaxation solution method for the discretized dual formulation of the signorini-coulomb contact problem. Comptes rendus de l'Academie des sciences - Serie I - Mathematique **333**(11), 1053–1058 (2001)
11. Cline, M.B., Pai, D.K.: Post-stabilization for rigid body simulation with contact and constraints. In: Proceedings of the IEEE International Conference in Robotics and Automation, IEEE, 2003
12. Cottle, R.W., Pan, J.-S., Stone, R.E.: The Linear Complementarity Problem. Academic Press, Boston, 1992
13. Cremer, J.F., Vanecek, G.: Building simulations for virtual environments. In: Proceedings of the IFIP International Workshop on Virtual Environments, Coimbra, Portugal, 1994

14. Dirkse, S., Ferris, M.: The PATH solver: A non-monotone stabilization scheme for mixed complementarity problems. Optim. Methods Softw. **5**, 123–156 (1995)
15. Dostal, Z., Haslinger, J., Kucers, R.: Implementation of the fixed-point method in contact problems with coulomb friction based on a dual splitting type technique. J. Com. Appl. Math. **140**, 245–256 (2002)
16. Glocker, C., Pfeiffer, F.: An lcp-approach for multibody systems with planar friction. In: Proceedings of the CMIS 92 Contact Mechanics Int. Symposium, Lausanne, Switzerland, 1992, pp. 13–30
17. Haslinger, J., Kucera, R., Dostal, Z.: On a splitting type algorithm for the numerical realization of contact problems with coulomb friction. Comput. Methods Appl. Mech. Eng. **191**, 2261–2281 (2002)
18. Haug, E.J.: Computer Aided Kinematics and Dynamics of Mechanical Systems. Allyn and Bacon, Boston, 1989
19. Kojima, M., Megiddo, N., Noma, T., Yoshise, A.: A unified approach to interior point algorithms for linear complementarity problems. Springer-Verlag, Berlin Heidelberg, 1991
20. Mangasarian, O.L.: Nonlinear Programming. McGraw-Hill, New York, 1969
21. Mangasarian, O.L., Fromovitz, S.: The fritz john necessary optimality conditions in the presence of equality constraints. J. Math. Anal. Appl. **17**, 34–47 (1967)
22. Miller, A., Christensen, H.I.: Implementation of multi-rigid-body dynamics within a robotics grasping simulator. In: IEEE International Conference on Robotics and Automation, 2003, to appear
23. Munson, T.S.: Algorithms and Environments for Complementarity. PhD thesis, Department of Computer Science, University of Wisconsin-Madison, Madison, Wisconsin, 2000
24. Necas, J., Jarusek, J., Haslinger, J.: On the solution of the variational inequality to the signorini problem with small friction. Bulletino U.M.I. **17B**, 796–811 (1980)
25. Panagiotopoulos, P.D.: Hemivariational Inequalities. Springer-Verlag, New York, 1993
26. Pang, J.-S., Stewart, D.E.: A unified approach to frictional contact problems. Int. J. Eng. Sci. **37**, 1747–1768 (1999)
27. Robinson, S.M.: Generalized equations and their solutions, part ii: Applications to nonlinear programming. Math. Progam. Study **19**, 200–221 (1982)
28. Rosato, A., Strandburg, K., Prinz, F., Swendsen, R.H.: Why the brazil nuts are on top: size segregation of particulate matter by shacking. Phys. Rev. Lett. **58**(10), 1038–1040 (1987)
29. Stewart, D.E.: Rigid-body dynamics with friction and impact. SIAM Rev. **42**(1), 3–39 (2000)
30. Stewart, D.E., Trinkle, J.C.: An implicit time-stepping scheme for rigid-body dynamics with inelastic collisions and coulomb friction. Int. J. Numer. Methods Eng. 39, 2673–2691 (1996)
31. Trinkle, J., Pang, J.-S., Sudarsky, S., Lo, G.: On dynamic multi-rigid-body contact problems with coulomb friction Zeithschrift fur Angewandte Mathematik und Mechanik **77**, 267–279 (1997)